EMTP-Based Model for Grounding System Analysis

Frank E. Menter, Member, IEEE
Technical University of Aachen
Aachen, Germany*)

Leonid Grcev, Member, IEEE
University of Skopje
Skopje, Republic of Macedonia

Abstract — **EMC and lightning protection analyses of large power systems require the knowledge of the dynamic behavior of extended grounding systems. They cannot be regarded as equipotential planes, but must be treated as coupling paths for transient overvoltages. This contribution presents a model for linear earth conductors based on the transmission line approach and outlines its integration in the transients program EMTP. Validation of the presented model is achieved by comparison with field measurements and with a rigorous electromagnetic model. Overvoltages and electrical fields throughout electrical power systems thus can be computed.**

KEYWORDS - Grounding Systems, Buried Conductors, EMC, Lightning Protection, Computer Modellling, Electromag netic Fields, EMTP

I. INTRODUCTION

Grounding systems serve two purposes: Firstly, their task is to disperse fault currents into the earth, which can be evoked either by internal, unbalanced faults or by external sources, such as lightning. Secondly, extended grounding systems create a reference potential for all electric and electronic apparatus making up a large-scale system. Local inequalities of this reference potential and disturbances conducted across the grounding system reportedly are a source of malfunction and destruction of components in electrical connection with the grounding system. This contribution treats grounding systems from the point of view of the electromagnetic compatibility (EMC) and thus regards a grounding system as a path of coupling between a source of interference, usually being an impressed fault or lightning current, and a consequence, typically a transient overvoltage or field stress, at the location of a disturbed object.

94 WM 135-4 PWRD A paper recommended and approved by the IEEE Substations Committee of the IEEE Power Engineering Society for presentation at the IEEE/PES 1994 Winter Meeting, New York, New York, January 30 - February 3, 1994. Manuscript submitted July 29, 1993; made available for printing December 22, 1993.

Since in most cases EMC studies require the knowledge of the system's performance over a wide frequency range, the presented methodology extends the range of validity of the well-known models for grounding systems towards higher frequencies in the order of magnitude of some megahertz. An approach could be based on the three basic concepts developed thus far. These are:

— *The Network Approach*, which models an earth conductor as equivalent π-circuits made up of lumped *R-L-C* elements. The coupling of earth conductors can be taken into account by mutually coupled inductances. Among others, Velazquez and Mukhedkar describe the procedure [1].

— *The Transmission Line Approach* was brought to practical applicability by Sunde [2]. The topology of the network of interconnected linear ground conductors is treated by the travelling wave technique pioneered by Bergeron. Nowadays, Papalexopoulos and Meliopoulos are basing their work on this method (e.g., [3]).

— *The Electromagnetic Field Approach* exhibits the most rigorous theoretical background of all three approaches. Strictly based on the theorems of electromagnetism and with the least neglects possible, the problems are defined in terms of retarded potentials, and among the possible strategies for their solution, the method of moments proved to be most efficient. Dawalibi could translate the highly complex relationships into practical, engineering programs [4].

For a model valid in the envisaged frequency range, the network approach was assumed not to be appropriate. In contrast, this contribution shall point out that the transmission line approach is a suitable and practical choice for the determination of both the transient ground potential rise and the electric fields in the vicinity of the grounding system. An existing program based on the electromagnetic field approach could validate this statement.

A brief review of Sunde's transmission line theory and the evaluation of the transmission line characteristics for common earth electrodes introduces this paper, followed by the description of an interface to the ATP version [5] of the wide-spread *Electromagnetic Transients Program* (EMTP) [6]. A post processor which computes electric fields in the soil from the current distribution in the

*) At present with SIEMENS AG, Transportation Systems, Erlangen, Germany

grounding system is sketched next, preceding the presentation of field measurements and of comparisons with a rigorous electromagnetic model. Finally, a lightning protection study for a 123 kV substation underlines the great advantage of not having just a stand-alone grounding systems program, but a tool capable of analyzing specific grounding systems in conjunction with the entire electrical system.

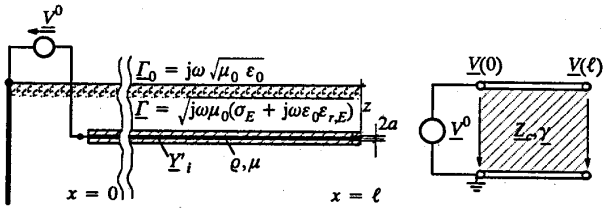

Fig. 1. Horizontal earth electrode and transition to an equivalent transmission line segment

II. Transmission Line Model For Buried Conductors

Fig. 1 illustrates the transition from a linear earth electrode to an equivalent transmission line with complex-valued, frequency dependent parameters $\underline{Z}_c(\omega)$ and $\underline{\gamma}(\omega)$, which denote the characteristic impedance and propagation function, respectively:

$$\underline{Z}_c(\omega) = \sqrt{\frac{\underline{Z}'(\omega)}{\underline{Y}'(\omega)}} \tag{1}$$

$$\underline{\gamma}(\omega) = \sqrt{\underline{Z}'(\omega)\cdot\underline{Y}'(\omega)} \tag{2}$$

The angular frequency, $\omega = 2\pi f$, uses f in Hz ($j = \sqrt{-1}$). This form corresponds to any two-conductor transmission line. Sunde derived equivalent expressions for a single conductor in contact to the soil, with the current returning through the earth. Both the longitudinal impedance per unit length, $\underline{Z}'$, and the transversal admittance per unit length, $\underline{Y}'$, of a horizontal conductor consist of an internal term and an earth return term in the following manner [2]:

$$\underline{Z}' \approx \underline{Z}_i' + \frac{j\omega\mu_0}{2\pi}\cdot\log\frac{1.85}{\sqrt{\underline{\gamma}^2 + \underline{\Gamma}^2}\cdot\sqrt{2az}} \tag{3}$$

$$\underline{Y}'^{-1} \approx \underline{Y}_i'^{-1} + \frac{1}{\pi(\sigma_E + j\omega\varepsilon_0\varepsilon_{r,E})}\cdot\log\frac{1.12}{\underline{\gamma}\cdot\sqrt{2az}} \tag{4}$$

Here, $\underline{Z}_i'$ denotes the internal impedance of a conductor of radius, a, buried at a depth, z, which is mainly governed by the skin effect, whereas $\underline{Y}_i'$ stands for the insulation admittance of an eventual coating, through which the conductor is in contact to the surrounding medium. The latter is characterized by the earth's conductivity, σ_E, relative permeability, $\varepsilon_{r,E}$, and permittivity, μ_0. All three lead to a propagation function,

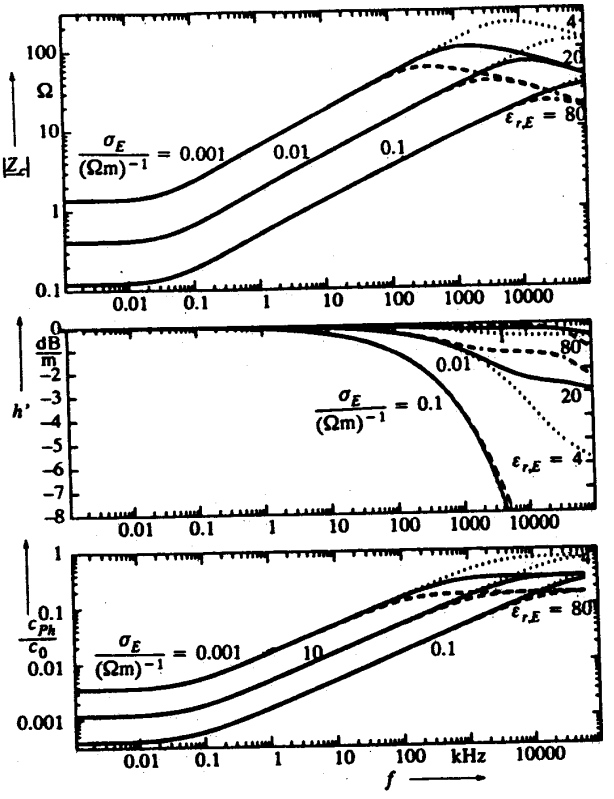

Fig. 2. Surge impedance, attenuation and phase velocity of a horizontal, bare copper wire (35 mm^2) buried at a depth of 0.5 m

$$\underline{\Gamma}(\omega) = \sqrt{j\omega\mu_0\cdot(\sigma_E + j\omega\varepsilon_0\varepsilon_{r,E})}\quad , \tag{5}$$

which would govern the transmission of impulses along the conductor if it were imbedded in a homogeneous soil with these parameters. Plumey, Kouteynikoff et al. derived analogous expressions for vertical ground rods [7], reading

$$\underline{Z}' \approx \underline{Z}_i' + \frac{j\omega\mu_0}{2\pi}\cdot\log\frac{1.12}{\sqrt{\underline{\gamma}^2 + \underline{\Gamma}^2}\cdot a} \tag{6}$$

$$\underline{Y}'^{-1} \approx \underline{Y}_i'^{-1} + \frac{1}{2\pi(\sigma_E + j\omega\varepsilon_0\varepsilon_{r,E})}\cdot\log\frac{\sqrt{\underline{\gamma}^2 + \underline{\Gamma}^2}\cdot a}{3.56} \tag{7}$$

Equation (2) together with (3) and (4) leads to a complex-valued, transcendent equation for the propagation function

$$\underline{\gamma} = \sqrt{\underline{Z}'(\underline{\gamma})\cdot\underline{Y}'(\underline{\gamma})}\quad , \tag{8}$$

which is repeatedly solved for all frequencies under investigation by means of a standard IMSL routine [8,9].

Fig. 2 shows the resulting quantities as functions of frequency for a variety of soil parameters σ_E and $\varepsilon_{r,E}$. It is

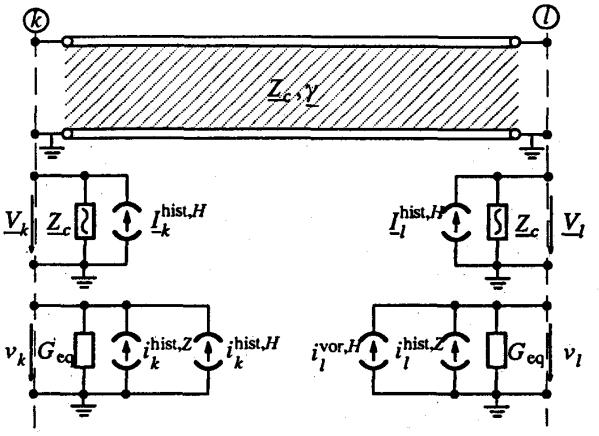

Fig. 3. Equivalent circuit for frequency-dependent transmission line

common engineering practice to express the propagation function in terms of transfer function, $\underline{H} = \exp\{-\underline{\gamma} \cdot \ell\}$, or attenuation per unit length, h', and phase velocity, c_{Ph}:

$$h'(\omega) = \frac{20\ \text{dB}}{\ell} \cdot \log|\underline{H}(\omega)| \cong -8.686\ \text{dB} \cdot \text{Re}\{\underline{\gamma}(\omega)\} \quad (9)$$

$$c_{Ph}(\omega) = \frac{\omega}{\text{Im}\{\underline{\gamma}(\omega)\}} \quad (10)$$

Only for lower frequencies, the properties of the ground are exclusively determined by the conductivity of the earth. Above some tens of kilohertz, its dielectric nature has to be taken into account.

III. Usage of EMTP for Grounding System Analysis

Once the characteristic impedance and the transfer function of linear earth conductors are known, any kind of extended grounding system can be modelled by a network of transmission line segments, provided that inductive and capacitive coupling between the different line segments can be neglected. At first sight, it is not evident that this assumption is permissible, but the purpose of this contribution is to show that for the grounding systems analyzed thus far, the resulting error is within acceptable limits. From an engineering point of view, the gained versatility and flexibility in modelling an actual earthing system together with live parts of the installation compensates the loss in accuracy.

A. Interface of the Ground Conductor Model to EMTP

Live and earthed parts of the electrical system are modelled by the Electromagnetic Transients Program. EMTP incorporates Bergeron's method for transmission lines, i. e. replacing the line by Thevenin equivalent circuits at both terminals, consisting of the constant and real-valued characteristic impedance and a current source for the history of the travelling waves with the travel time τ (Fig. 3, upper index/sign for forward travelling wave, lower index/sign for backward travelling wave):

$$i_{k\ l}^{hist}(t) = \frac{1}{Z_c} \cdot v_{k\ l}(t-\tau) \pm i_{k\ l}(t-\tau) \quad (11)$$

In the frequency domain, the transition to complex-valued, frequency-dependent parameters necessary for earth conductors is simply,

$$\underline{I}_{k\ l}^{hist,H} = \underline{H} \cdot (\underline{Z}_c^{-1} \cdot \underline{V}_{k\ l} \pm \underline{I}_{k\ l}) \ , \quad (12)$$

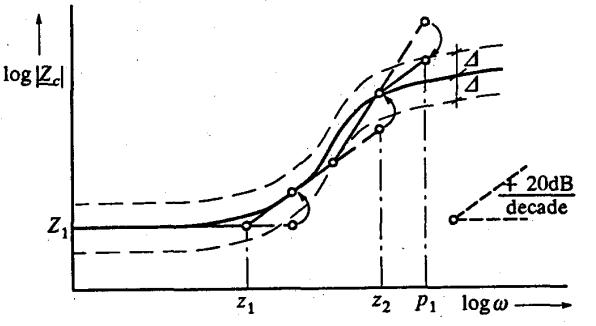

Fig. 4-a. Marti's strategy of approximation applied to the modulus of the characteristic impedance

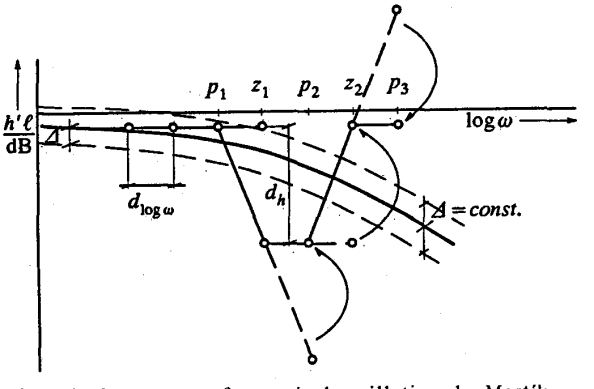

Fig. 4-b. Occurrence of numerical oscillations by Marti's strategy if applied to the attenuation

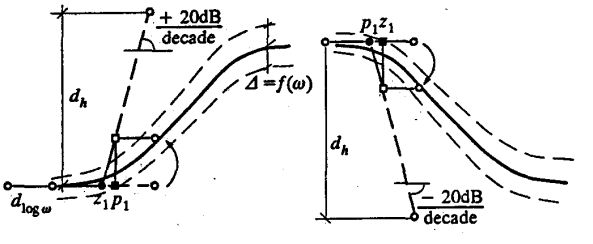

Fig. 4-c. Remedy by modified strategy (cf. text)

but since EMTP works in the time domain, the back transformation leads to two nested convolution integrals:

$$i_k^{hist,H}(t) = h_\delta(t) * [\mathcal{F}^{-1}\{\underline{Z}_c^{-1}(\omega)\} * v_k(t) \pm i_k(t)] \qquad (13)$$

The numerical effort for the convolutions can be reduced drastically if the technique of the so-called recursive convolution can be applied [10]. For this purpose, it is necessary to approximate the characteristic impedance and the transfer function by rational functions, i. e. it is mandatory to identify their poles and zeroes. Martí's original strategy ([11], Fig. 4-a) of proceeding form lower to higher frequencies in a log-log-chart and placing a pole or zero wherever an asymptotic approximation leaves a tolerance strip of width 2Δ is not adequate in the present case: In contrast to its original field of application, observed frequency, characteristic impedance and attenuation cover several orders of magnitude, and thus frequently cause numerical oscillations (Fig. 4-b).

A remedy could be found by the introduction of a relative error criterion for the tolerance strip and by the possibility of placing closely adjacent pole/zero-pairs in order to jump exactly on the target function ([12], Fig. 4-c).

B. Modelling the Soil Ionization with EMTP

If large current densities emanate from the conductor into the soil, the critical field strength can be exceeded and breakdowns occur. Then, the conductor will be surrounded by a cylindrical corona-type discharge pattern, which augments the available surface for the transition of the current from the conductor to the earth. The breakdown strength, E_{crit}, of the soil is a function of its conductivity, measurements [13] lead to the empirical formula

$$E_{crit} = 241 \cdot \sigma_E^{-0.215} \qquad (14)$$

for E_{crit} in kV/m and the soil conductivity, σ_E, in $(\Omega m)^{-1}$. The distance from the center of the earth conductor at which the ionization of the soil ceases, may be regarded as an effective radius. Ohm's law governs the relationship between current density at a distance, a, from the conductor and field in the soil,

$$\frac{\partial i / \partial x}{2\pi a} = \sigma_E \cdot E \quad . \qquad (15)$$

The combination of the two latter expression for $a = a_{eff}$ and $E = E_{crit}$ yields

$$a_{eff} = \frac{1}{2\pi \cdot 241} \cdot \frac{\partial i}{\partial x} \cdot \sigma_E^{-0.785} \qquad (16)$$

for the effective radius, a_{eff}, in m, and the leakage current per unit length, $\partial i/\partial x$, in kA/m. The seemingly increased circumference of the conductor will affect only the transversal admittance, $\underline{Y}'(\partial i/\partial x)$, whereas the by far most part of the longitudinal current will stay within the conductor: the longitudinal impedance, $\underline{Z}'$, remains unchanged by ionization phenomena.

The basic idea of incorporating an ionization model into the simulation network is to concentrate that part of the transversal admittance, $\Delta\underline{Y}'(\partial i/\partial x)$, which exceeds the value disregarding the ionization, $\underline{Y}_0'$, at the intersections of transmission line segments, which can be generated without the necessity of taking the soil ionization into account (Fig. 5).

The implementation of the model makes use of the observation that the additional transverse admittance, $\Delta\underline{Y}'(\omega, \partial i/\partial x)$, can be decomposed into

$$\Delta\underline{Y}'(\partial i / \partial x, \omega) \approx \kappa(\partial i / \partial x) \cdot \Delta\underline{Y}_1'(\omega) \quad , \qquad (17)$$

where $\Delta\underline{Y}_1'$ is a specific fundamental function and κ is a multiplier, only depending on the leakage current. Both functions can be determined by formal variations of ω and $\partial i/\partial x$ before the simulation run. At the beginning of the run, $\Delta\underline{Y}_1'$ is similarly approximated by its poles and zeroes, which are passed to EMTP's *laplace xform* module for the representation of arbitrary, frequency dependent impedances. During the run, the additional transversal admittances are scaled by the multiplier κ, whose locally valid actual argument, $\partial i/\partial x(x)$, is determined at each time step from the difference of the longitudinal currents and the length, ℓ, of the corresponding transmission line segment. These run-time evaluations, the interpolation on the pointlist function $\kappa(\partial i/\partial x)$ and the scaling of all elements $\Delta\underline{Y}_1'$ is performed by the recently developed tool *models* of the ATP version of EMTP [14,15].

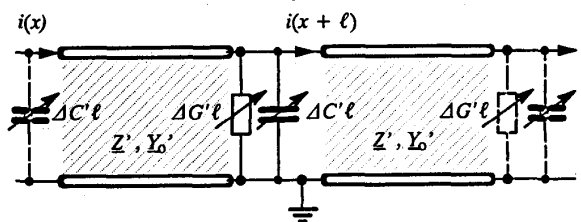

Fig. 5. Leakage current controlled lumped elements to model soil ionization

IV. Computation of the Electric Field Distribution

Considering the possibility to extend the application of the developed model to EMC studies, the electric field vector is chosen as a key quantity. The main reason for this is the well known fact that in the general case the voltage between points along specified path is not equal to the potential difference, but is defined as a line integral of the electric field vector along the path. In order to compute the electric field distribution in the vicinity of the grounding system, a post processor to EMTP has been developed. Since the grounding system is modelled as a

network of arbitrarily connected or disconnected straight thin conductors, the electric field can be computed as a superposition of the contributions of field-generating currents on all straight conductors, which are readily available as EMTP results.

Usually, in order to avoid complications in the solution, only the electric charge distribution in the grounding system conductors is considered as a source of the electric field. This is equivalent to consider only the leakage currents from the conductors in the evaluation of the electric field and the voltages [16]. In other words, this simplification is based on the neglect of the time-varying longitudinal current in the ground conductors as an additional source of the electric field. But it has been shown [17] that such simplification can lead to extremely wrong results in the computation of voltages. The procedure used here takes into account both components of the electric field, due to the electric charges and longitudinal current distribution in all the ground conductors.

In this study, a frequency-domain approach is used, i.e. fields are computed from the steady-state current distribution for $f = 0 \ldots 1$ MHz. This yields the transfer function for the electric field at prescribed observation points in the vicinity of the grounding system. Such transfer functions subsequently can be Fourier transformed to obtain the time-domain response.

Grounding conductors are divided in a number of smaller segments in the EMTP and the longitudinal currents are determined only in the end or junction points of the segments. The current in all other points can be determined by interpolation. Among the many choices for the interpolating function, one is exceptionally attractive for our purposes: the so called piecewise sinusoidal approximation of the current distribution $\underline{I}(\ell)$ that can be expressed by:

$$\underline{I}(\ell) = \sum_{k=1}^{N} \frac{P_k(\ell)}{\sinh(\underline{\Gamma} d_k)} \left\{ \underline{I}_k^- \sinh\left[\underline{\Gamma}\left(\ell_k^- - \ell\right)\right] + \underline{I}_k^+ \sinh\left[\underline{\Gamma}\left(\ell - \ell_k^+\right)\right] \right\} \tag{18}$$

$\underline{\Gamma}$ is explained above (5), and $P_k(\ell)$ are unit pulse functions with the values

$$P_k(\ell) = \begin{cases} 1, & \ell_k^- \le \ell \le \ell_k^+ \\ 0, & \text{elsewhere} \end{cases} \tag{19}$$

Here, ℓ denote points along the axis of the conductors, ℓ^-_k is the first, ℓ^+_k is the second end point and d_k is the length of the k-th segment. $\underline{I}^-_k$ and $\underline{I}^+_k$ are current phasors at the first and the second end point of the k-th segment, respectively.

The main reason for the approximation of the current with sinusoidal functions on the segments (18) is to exploit their properties revealed by Schelkunoff [18]. The sinusoidal line current source is probably the only finite source with simple and exact closed form expressions for the near fields [19]. In this study, the influence of the interface between the air and the earth is taken into account approximately by the modified image theory [16].

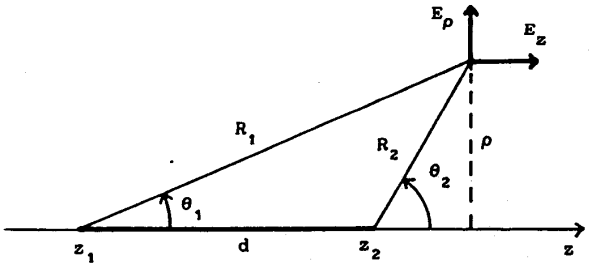

Fig. 6. Computation of the electric field distribution

By this way the electric field at a point in the earth due to the sinusoidal sources on the k-th segment is obtained by superposition of the field of the original and image sinusoidal sources both placed in the unbounded conducting medium. The exact expressions for the electric field in a local cylindrical co-ordinate system illustrated in Fig. 6, due to the current distribution given in (18) on the k-th segment at a near point are:

$$\underline{E}_{k\rho} = \frac{\underline{\eta}}{4\pi\rho\sinh(\underline{\Gamma} d_k)} \Big[\left(\underline{I}_k^- e^{-\underline{\Gamma} R_1} - \underline{I}_k^+ e^{-\underline{\Gamma} R_2}\right)\sinh\underline{\Gamma} d_k + \left(\underline{I}_k^- \cosh\underline{\Gamma} d_k - \underline{I}_k^+\right) e^{-\underline{\Gamma} R_1} \cos\theta_1 + \left(\underline{I}_k^+ \cosh\underline{\Gamma} d_k - \underline{I}_k^-\right) e^{-\underline{\Gamma} R_2} \cos\theta_2 \Big]$$

$$\underline{E}_{kz} = \frac{\underline{\eta}}{4\pi\sinh\underline{\Gamma} d_k} \Big[\left(\underline{I}_k^- - \underline{I}_k^+ \cosh\underline{\Gamma} d_k\right) \frac{e^{-\underline{\Gamma} R_2}}{R_2} + \left(\underline{I}_k^+ - \underline{I}_k^- \cosh\underline{\Gamma} d_k\right) \frac{e^{-\underline{\Gamma} R_1}}{R_1} \Big] \tag{20}$$

where $\underline{\eta}$ is the intrinsic impedance of the medium:

$$\underline{\eta} = \sqrt{\frac{j\omega\mu_0}{j\omega\varepsilon_0\varepsilon_{r,E} - \sigma_E}} \tag{21}$$

The various geometrical quantities are illustrated in Fig. 6. The references concerning the derivation of (20) can be found elsewhere [19].

A brief description of the steps involved in the derivation are included in the Appendix for completeness.

V. Verification and Application

A. Comparison with Field Measurements by EDF

The Direction des Études et Recherches of the Électricité de France granted an insight in their recordings of extensive field measurements performed in the mid-80's [20]. Impulse currents with front times down to 0.2 μs have been fed into single- and multi-conductor earthing arrangements as used industrially. The resulting

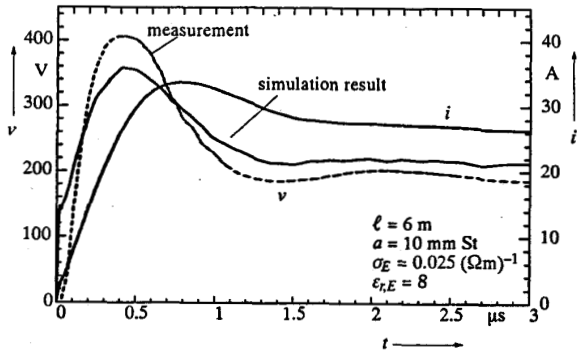

Fig. 7. Measured and calculated ground potential rise of a ground rod

transient ground potential rise has been measured by means of a 60 m long ohmic divider, still having a measuring bandwidth of 3 MHz.

Fig. 7 shows the oscillograms of voltage and current as recorded on a ground rod (steel, 20 mm in diameter, other parameters in the figure). Included in the figure is the simulation result of the voltage when a current according to the measured one is impressed in the corresponding transmission line segment. The peak of the measured voltage curve is always higher than the corresponding value of the simulation, which can be explained by some remaining inductive voltage drop during the wave front along the divider added to the actual potential rise at the clamp of the ground rod.

The effective grounding impedance (Fig. 8) has been determined by a division of the Fast Fourier Transforms of measured voltage and current on a 10 m long horizontal ground wire made of copper alloy. The corresponding simulation curve has been generated by EMTP's frequency scan option, requesting a repeated set of phasor solutions of the simulation network. The curves show good agreement up to frequencies of 1 MHz, the underestimation at higher frequencies may be explained by the above-mentioned effect.

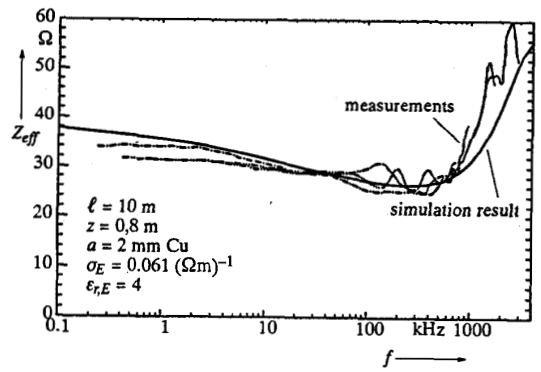

Fig. 8. Measured and calculated effective grounding impedance of a horizontal earth conductor

More complex grounding arrangements have been studied, too. Fig. 9 depicts the results in time domain of a tower footing, consisting of a set of four ground rods and two square loops (6 m × 6 m) in 1 m and 4 m depth, respectively. Except for a 200 ns long period during the wave front, the agreement between measurement and simulation is satisfactory.

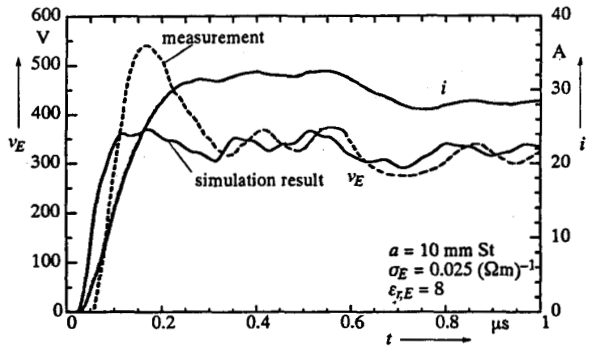

Fig. 9. Measured and calculated ground potential rise of a tower footing

B. Comparison with a Rigorous Electromagnetic Model

As an example, a grid-type grounding system of 10 m × 10 m with 3 × 3 meshes has been studied. A sinusoidal current of 1 kA and variable frequency is fed into the slightly asymmetric arrangement at its center ((*x*;*y*) = (5 m;5 m)), the first regular mesh branch being reached at (*x*;*y*) = (5 m;6.67 m). The conductors have a diameter of 10 mm, are assumed to be of ideal conductivity and are buried at a depth of 0.5 m in a soil with $\sigma_E = 0.01\ (\Omega m)^{-1}$ and $\varepsilon_{r,E} = 1$.

Since the local distribution of longitudinal and leakage currents within the grounding system is only an intermediate quantity in the computation of touch and step voltages above the grounding system, a comparison of the resulting electric fields at the earth's surface has been performed. Firstly, the current distribution in the grounding system according to the transmission line approach outlined above has been taken as input to the post processor described in section IV. The resulting field distribution is compared to a second, independent computation according to the rigorous electromagnetic approach developed by the second author [21]. The results are compared in Fig. 10.

The transmission line model slightly overestimates the results of the rigorous model, which is taken as a reference here. But still the interesting phenomena are modelled correctly, and the results are obtained within a fraction of the computation time required for the rigorous approach.

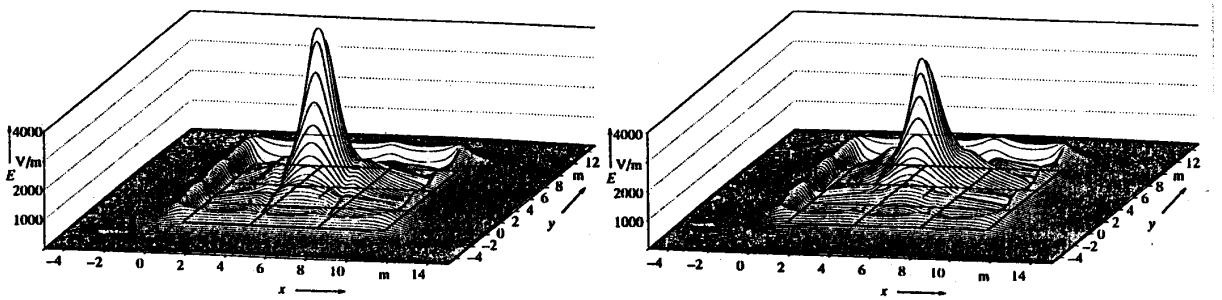

Fig. 10. Field distribution above a mesh-type grounding system. Comparison for $f = 1$ MHz of the transmission line approach (left) and the rigorous electromagnetic approach (right)

C. Lightning Protection study for a 123 kV substation

This application example sketches the procedure and results of a lightning protection study for a 123 kV substation. The lightning is assumed to hit the third tower of an overhead line (Fig. 11) and should have a crest value of 200 kA and an impulse shape as recommended in [22]. The EMTP data deck for the two-system, three-phase overhead line as well as the representation of the switchyard (voltage transformers, surge arresters, busbars and power transformer) has been made available by a CIGRÉ working group [23]. It has been combined with a detailed description of the tower footings and the meshed grounding system of the switchyard (70 m × 50 m) by means of the transmission line model.

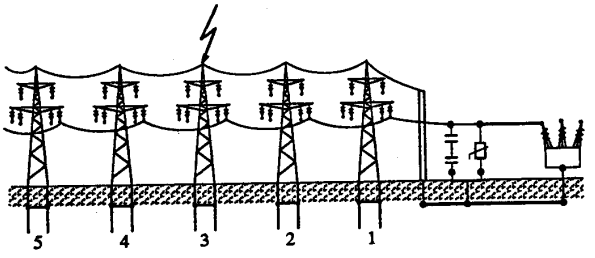

Fig. 11. Lightning-struck overhead line entering 123 kV substation

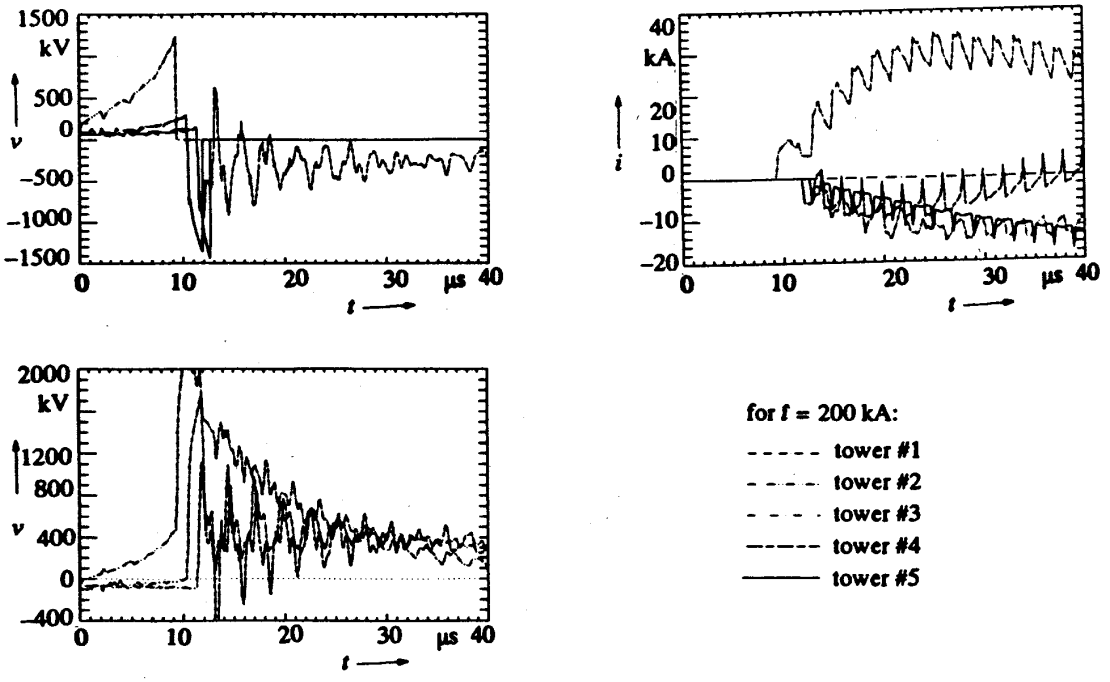

Fig. 12. Voltages and currents across insulators, and conductor potential at towers #1...#5 for phase A.

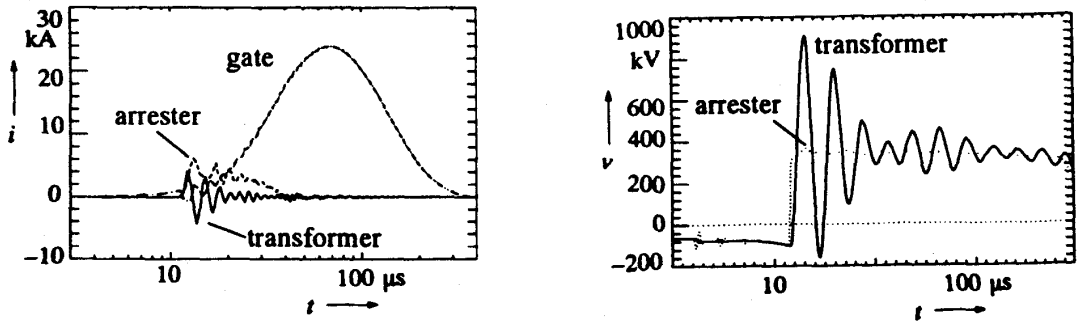

Fig. 13. Currents injected in the earthing system and voltages across transformer and arrester terminals,

The employed time-dependent flashover model leads to the fact that, as a consequence of the lightning stroke to tower #3, backflashovers occur at the towers #2, #4 and #5, whereas the flashover at tower #3 impresses a portion of the lightning current into the phase conductor (Fig. 12). Within the substation (Fig. 13), an oscillating overvoltage of nearly 9 p.u. very probably will destroy the power transformer windings. The metal oxide arrester (v_{max}=3.5 p.u.) has been placed at too large a distance from the transformer to provide sufficient protection. Under such fault conditions, currents are impressed at different locations into the grounding system, the major part of which through the foundation of the gate to which the neutral conductor of the overhead line is connected. This situation results in considerable local variations of the transient ground potential rise, temporarily reaching 100 kV. Such potential differences within the grounding system are able to cause EMC problems, if, for example, the shield of a measuring cable between voltage transformer and relaying room is grounded at both ends. Then, a rapidly varying current will flow on the cable shield and crosstalk will occur onto secondary circuits.

VI. Conclusion

Lightning protection and EMC analyses of power electric systems paying special attention to the grounding conditions require the knowledge of the dynamic properties of ground conductors and extended earthing systems. For this purpose, a methodology has been developed which is based on a transmission line approach for linear ground conductors. Thus, it is the possible to integrate the grounding system as a network of such conductors into EMTP. The necessary interface algorithm has been outlined as well as a post processor capable of deriving electrical fields in the vicinity of the grounding system. Validation of the method developed by the first author could be achieved by means of comparisons with field measurements by the EDF at Paris, France, and with computational results produced by the second author's code based on a rigorous electromagnetic field approach. As an example, some aspects of a lightning protection study for a 123 kV substation have been selected in order to underline the versatility and flexibility of the proposed method, capable of modelling not only the grounding system itself, but also the electrical apparatus connected to it.

VII. Acknowledgements

Financial support of the project had been granted by the Deutsche Forschungsgemeinschaft, Bonn, Germany, which is gratefully appreciated. Messrs. Hervé Rochereau of EDF, Paris, France and Vincent Vanderstockt of LABORELEC, Brussels, Belgium, amiably made available the measurement and substation data, respectively.

The fist author wishes to express his gratitude to his academic teacher, Prof. Dr. Klaus Möller. Under his supervision, the Ph.D. thesis could be realized upon which parts of the present contribution are based.

VIII. References

[1] R. Velazquez and D. Mukhedkar, "Analytical modelling of grounding electrodes transient behavior," *IEEE Trans. Power Apparatus and Systems*, vol. 103, 1984, pp. 1314-1322.

[2] E. D. Sunde, *Earth conduction effects in transmission systems*, 2nd ed., New York: Dover Publications, 1968.

[3] A. D. Papalexopoulos and A. P. Meliopoulos, "Frequency dependent characteristics of grounding systems," *IEEE Trans. Power Delivery*, vol. 2, October 1987, pp. 1073-1081.

[4] F. Dawalibi and A. Selbi, "Electromagnetic Fields of Energized Conductors," *IEEE/PES 1992 Summer Meeting*, Paper 92 SM 456-4 PWRD.

[5] D. van Dommelen [ed.], *Alternative Transients Program — Rule Book*, Leuven EMTP Center, Catholic University of Leuven, Belgium; July 1987.

[6] W. Long, D. Cotcher, D. Ruiu, P. Adam, S. Lee, and R. Adapa, "EMTP — A powerful tool for analyzing power system transients," *IEEE Trans. Computer Application in Power*, July 1990, pp. 36-41.

[7] J. P. Plumey, D. J. Robertou, J. M. Fontaine, and P. Kouteynikoff, "Impédance haute fréquence d'une antenne déposée dans un demi-espace conducteur," *Proc. Colloque sur la Compatibilité Électromagnétique*, paper C.1, Trégastel, France; January 1981.

[8] IMSL, Inc., *IMSL Reference manual*, 8th ed.; Houston, TX: IMSL, 1980.

[9] P. Wolfe, "The secant method for simultaneous nonlinear equations," *Communications of the ACM*, vol. 2, 1959.

[10] A. Semlyen and A. Dabuleanu, "Fast and accurate switching transients calculations on transmission lines with ground return using recursive convolutions," *IEEE Trans. Power Apparatus and Systems*, vol. 94, 1975, pp. 561-571.

[11] J. R. Martí, "Accurate modelling of frequency-dependent transmission lines in electromagnetic transient simulations," *IEEE Trans. Power Apparatus and Systems*, vol. 101, 1982, pp. 147-155.

[12] F. Menter, "Accurate modelling of conductors imbedded in earth with frequency-dependent distributed parameter lines," *Proceedings of the 21st EMTP User Group Meeting*, paper 92.09, Kolymbari, Greece; Athens: National Technical University, June 1992.

[13] E. E. Oettle, "A new general estimation curve for predicting the impulse impedance of concentrated earth electrodes," *IEEE/PES 1987 Winter Meeting*, Paper 87 WM 567-1 PWRD.

[14] L. Dubé and I. Bonfanti, "MODELS, a new simulation tool in EMTP," *European Transactions on Energy and Power (ETEP)*, vol. 2, 1992, pp. 45-50.

[15] F. Menter, *Computation of electromagnetic transients in extended grounding systems (in German)*, Ph.D. thesis, Technical University of Aachen; Aachen: Shaker 1993.

[16] T. Takashima, T. Nakae, and R. Ishibashi, "High Frequency Characteristics of Impedances to Ground and Field Distributions of Ground Electrodes," *IEEE Trans. Power Apparatus and Systems*, Vol. 100, 1980, pp. 1893-1900.

[17] L. Grcev, "Computation of Transient Voltages near Complex Grounding Systems Caused by Lightning Currents," *IEEE 1992 International Symposium on Electromagnetic Compatibility*; Anaheim, CA, pp. 393-400.

[18] S. A. Schelkunoff and H. T. Friis, *Antennas, Theory and Practice*, New York: Wiley, 1952, p. 401.

[19] D. V. Otto and J. H. Richmond, "Rigorous Field Expressions for Piecewise-Sinusoidal Line Sources," *IEEE Trans. Antennas and Propagation*, Vol. 17, 1969, p. 98.

[20] H. Rochereau, "Comportement des prises de terre localisées parcourues par des courants à front raide," *EDF Bulletin de la Direction des Études et Recherches*, série B, no. 2, 1988, pp. 13-22.

[21] L. Grcev and F. Dawalibi, "An electromagnetic model for transients in grounding systems," *IEEE Trans. Power Delivery*, vol. 5, 1990, pp. 1773-1781.

[22] CIGRÉ working group 33.01, *Guide to procedures for estimating the lightning performance of transmission lines*, Guide no. 63, Paris: CIGRÉ, October 1991.

[23] V. Vanderstockt, *Application procedures for station insulation co-ordination*, IWD7 SC 33-92 (WG11), Paris: CIGRÉ, May 1992

[24] J. H. Richmond, *Computer Analysis of Three-Dimensional Wire Antennas*, Technical Report 2708-4, ElectroScience Laboratory, Ohio State University, 1969.

APPENDIX

The derivation in this Appendix is based on [18] and [24]. Acccording to the fundamental analysis [24], the z-component of the electric field vector of the line source with arbitrary current distribution illustrated in Fig. 6 is given by:

$$\underline{E}_z = \frac{1}{j\omega \underline{\varepsilon}} \int_{z_1}^{z_2} \left(\frac{\partial^2 \underline{g}}{\partial^2 z} - \underline{\Gamma}^2 \underline{g} \right) \underline{I}(z')\, dz' \tag{A1}$$

with

$$\underline{\varepsilon} = \varepsilon_0 \varepsilon_{r,E} + \frac{\sigma_E}{j\omega}, \quad \underline{g} = \frac{\exp(-\underline{\Gamma} r)}{4\pi r}, \quad r = \sqrt{\rho^2 + (z - z')^2}$$

Noting that

$$\frac{\partial \underline{g}}{\partial z} = -\frac{\partial \underline{g}}{\partial z'}, \qquad \frac{\partial^2 \underline{g}}{\partial z^2} = \frac{\partial^2 \underline{g}}{\partial z'^2} \tag{A2}$$

and integrating the first term in (A1) by parts twice and substituting (A2) in (A1) we have:

$$\underline{E}_z = -\frac{1}{j\omega \underline{\varepsilon}} \left[\underline{I}'(z') \underline{g} + \underline{I}(z') \frac{\partial \underline{g}}{\partial z} \right]_{z' = z_1}^{z' = z_2} + \frac{1}{j\omega \underline{\varepsilon}} \int_{z_1}^{z_2} \left[\frac{d^2 \underline{I}(z')}{dz'^2} - \underline{\Gamma}^2 \underline{I}(z') \right] \underline{g}\, dz' \tag{A3}$$

If the current between $z'=z_1$ and $z'=z_2$ is of form

$$\underline{I}_k(z) = A\cosh\underline{\Gamma}z + B\sinh\underline{\Gamma}z \quad , \tag{A4}$$

the bracketed expression in the integrand of (A3) vanishes. Hence:

$$\underline{E}_z = \frac{1}{4\pi j\omega\underline{\varepsilon}}\left[\frac{\underline{I}'(z_1)e^{-\underline{\Gamma}R_1}}{R_1} - \frac{\underline{I}'(z_2)e^{-\underline{\Gamma}R_2}}{R_2} + \underline{I}(z_2)\frac{\partial}{\partial z}\frac{e^{-\underline{\Gamma}R_2}}{R_2} - \underline{I}(z_2)\frac{\partial}{\partial z}\frac{e^{-\underline{\Gamma}R_1}}{R_1}\right] \tag{A5}$$

where $\underline{I}'(z_1)$ and $\underline{I}'(z_2)$ denote the derivatives of the current at the end points. The constants A and B can be eliminated to express the current distribution in terms of the endpoint currents $\underline{I}(z_1)$ and $\underline{I}(z_2)$ as follows:

$$\underline{I}(z) = \frac{1}{\sinh\underline{\Gamma}d_k}\left[\underline{I}(z_1)\sinh\underline{\Gamma}(z_2 - z) + \underline{I}(z_2)\sinh\underline{\Gamma}(z - z_1)\right] \tag{A6}$$

From (A6):

$$\underline{I}'(z_1) = \frac{\underline{\Gamma}}{\sinh\underline{\Gamma}d_k}\left[\underline{I}(z_2) - \underline{I}(z_1)\cosh\underline{\Gamma}d_k\right] \tag{A7}$$

$$\underline{I}'(z_2) = \frac{\underline{\Gamma}}{\sinh\underline{\Gamma}d_k}\left[\underline{I}(z_2)\cosh\underline{\Gamma}d_k - \underline{I}(z_1)\right] \tag{A8}$$

Equations (A5) to (A8) yield the z-component of the electric field in (18). This expression excludes the field contributions from the point charges at the endpoints of the line segments, since these charges disappear when two segments are connected. Such charges are also neglected in case of a segment with no connected end point. It is assumed that the longitudinal current at the open endpoint is zero. Since the point charges there are equal to $-\underline{I}/j\omega$, they are also zero. It should be noted that this assumption only applies on the longitudinal current at the segment's open endpoint and not on the radial or leakage current.

The same procedure can be repeated for the ρ-component of the electric field. This will yield:

$$\underline{E}_\rho = \frac{\underline{\eta}}{4\pi\rho}\left\{\left[\underline{I}'(z_2)\cos\theta_2 - \underline{\Gamma}\underline{I}(z_1)\right]e^{-\underline{\Gamma}R_2} - \left[\underline{I}'(z_1)\cos\theta_1 - \underline{\Gamma}\underline{I}(z_2)\right]e^{-\underline{\Gamma}R_1}\right\} \tag{A9}$$

The ρ-component of the electric field in (18) follows from (A9) and (A6) to (A8).

Dr. Frank E. Menter (M 93) was born in Essen, Germany, on August 14, 1963. He graduated from the Rheinisch-Westfälische Technische Hochschule in Aachen, Germany, and received the Dipl.-Ing. degree. His practical experiences include various stays with Siemens AG, Nixdorf Computers and the Research Laboratory of Hitachi Cable, Inc. As a scientific assistant at the Institute for HighVoltage Engineering at Aachen University, he worked as a project co-ordinator of two larger projects, the first of which resulting in a lightning protection scheme for DC driven urban railways and the second treating EMC problems of high voltage switchgears. In May 1993, he received the doctoral Dr.-Ing. degree from the same University.

Currently, he is with Siemens Transportation Systems at Erlangen, Germany. In the Traction Power Supply Department, he is concerned with grounding and EMC problems. Dr. Menter is a member of the IEEE Power Engineering Society and the VDE.

Dr. Leonid Grcev (M 84) was born in Skopje, Macedonia on April 28, 1951. He received Dipl. Ing. degree from the University of Skopje, and the M.Sc. and Ph.D. degrees from the University of Zagreb, Croatia, all in Electrical Engineering, in 1978, 1982 and 1986, respectively. From 1978 to 1988, he held a position with the Electric Power Company of Macedonia, Skopje, working in the Telecommunication and Information Systems Departments. He worked on a number of projects involving radio systems, PLC and electromagnetic compatibility related problems and specialized computer software development. He was a Head of the Information System Department from 1985. In 1988, he joined the Faculty of Electrical Engineering at the University of Skopje, and is now an Associate Professor of Electrical Engineering. His present research interests are in computational electromagnetics applied to grounding and interference.

Dr. Grcev is a member of IEEE PE, AP, MTT, EMC, MAG and EI Societies. He is also a member of the Applied Computational Electromagnetic Society.

DISCUSSION

Abdul M. Mousa (B.C. Hydro, Vancouver, Canada. I wish to congratulate Dr. Menter and Dr. Grcev for an interesting paper. My comments pertain to soil ionization, a factor which is significant in case of concentrated electrodes, especially where soil resistivity is high. In this connection, it should be noted that Oettle's work [13] has been superseded by Mousa's recent paper [25]. The main findings as they pertain to this paper are as follows:

1. The mechanism of breakdown of the soil indicates that **no** direct correlation exists between the ionization gradient E_{crit} and the resistivity ρ (or the conductivity) of the soil. That fact is proven by the scatter in the relation between E_{crit} and ρ observed by Oettle [26]. Please see Fig. 14.

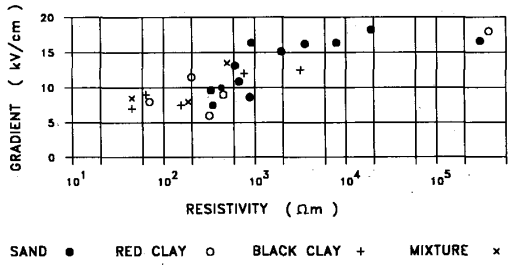

Fig.14. Relation between the ionization gradient and resistivity of the soil according to Oettle.

2. E_{crit} is mainly governed by the water content of the soil.
3. Due to inhomogeneity of the soil, E_{crit} varies from point to point along the electrode. The **effective** value of E_{crit} is **not the average** of the subject values, but is rather **equal to the minimum** value encountered along the electrode.
4. For practical applications, the value of the ionization gradient should be taken equal to 300 kV/m. Based on the above, equations (14) and (16) should be replaced by:

$$E_{crit} = 300 \text{ kV/m} \qquad ...(14.1)$$

$$a_{eff} = (\rho/600\pi)\,(\partial i/\partial x) \qquad ...(16.1)$$

where $(\partial i/\partial x)$ is in kA/m, and ρ is in Ωm.

5. With typical water content, the value of the relative permittivity of the soil should be around 10 or even higher. The values shown in Figs. 7 and 8 are reasonable. On the other hand the value 1 used in part B of Section V is not realistic.
6. It should be noted that soil ionization was not present in the examples given in Figs. 7 and 9, because the amplitudes of the currents were too small. In the case of Fig. 7 in which a 6 m long rod is located in a soil having $\rho = 40$ Ωm , the minimum current needed to initiate ionization would be as follows:

   a) About 1.4 KA if eqn. (14.1) is used.
   b) About 2.5 KA if eqn. (14) is used.

   The actual current, on the other hand, was only about 30 A.

REFERENCES

[25] A.M. Mousa, "The Soil Ionization Gradient Associated with Discharge of High Currents into Concentrated Electrodes", **IEEE Paper** No. 94 WM 078-6 PWRD.

[26] E.E. Oettle, "The Characteristics of Electrical Breakdown and Ionization Processes in Soil", **Trans. of the South African IEE**, pp. 63-70, December 1988.

Manuscript received February 22, 1994.

F.P. DAWALIBI, Safe Engineering Services & technologies ltd., Montreal, Quebec, Canada, H3M 1G4. The authors should be commended for an excellent paper illustrating the use of transmission line theory and its integration with the EMTP transient program. There is an urgent need for technical contributions in the area of transient performance of grounding systems in order to help refine the various analytical methods in use and determine the domain of their validity by comparing their computation results.

One major simplification of this transmission line approach is the neglect of the inductive, capacitive and perhaps the conductive coupling between the conductor segments of the ground network. According to the authors, this neglect does not lead to significant errors. This conclusion may not be valid at all frequencies and for all ground grid configurations. Indeed our own investigations [1,2] have revealed that coupling from aboveground conductors and loops may affect results even at low frequencies. Is the authors' conclusion based on extensive simulations or simply the result of a limited number of tests on simple ground configurations?

[1] F.P. Dawalibi, W.K. Daily, "Measurements and Computations of Electromagnetic Fields in Electric Power Substations," Paper No. 93 WM 220-0 PWRD T-PWRD, Presented at IEEE PES 1993 Winter Meeting in New York, New York.

[2] W. Xiong, F.P. Dawalibi, "Transient Performance of Substation Grounding Systems Subjected to Lightning and Similar Surge Currents," Paper No. 94 WM 139-6 PWRD, Presented at IEEE PES 1994 Winter Meeting in New York, New York.

Manuscript received February 22, 1994.

DR. FRANK E. MENTER, PROF. DR. LEONID GRCEV: The authors thank Messrs. A. M. Mousa and F. P. Dawalibi for their kind words. We are especially grateful to Mr. Abdul M. Mousa for his discussion, which enhanced the quality of our paper. His remarks on recent findings in the experimental analysis of breakdown phenomena are appreciated. Since we did not perform such analyses ourselves, we had to adopt one model available though the literature. So, we chose Oettle's model which lead to equations (14) and (16). Since the model Mr. Mousa now proposes (eqns. (14.1), (16.1)) is even less complicated, its introduction is feasible and we are delighted to incorporate his suggestion into our procedures.

Regarding the questions raised by Mr. Farid F. Dawalibi, it should be noted that the aim of this paper was to demonstrate that the transmission line approach for grounding system analysis integrated within the EMTP could lead to practically useful results. The authors' conclusion for the accuracy of the results is based on comparisons with field measurements performed by the EDF, Paris, France. An extensive set of experiments had been performed in Les Renardières in 1976-78 and in St-Brieuc in 1985. All experiments had been repeated to cover any seasonal and weather effects. Among the grounding arrangemets under study were vertical ground rods, horizontal earth electrodes, hemispheres, grids, star- and serpentine-shaped electrodes and tower footings. Further reference on the measurements can be found in [20]. The comparison has been performed in Paris in 1992/93 and has been documented in [15]. However, it is true that the investigated earthing structures do not include larger grids; the validation for such structures has been achieved by comparison with a separate program developed by the second author, implementing a rigorous electrodynamic approach. Additional checks and analyses of large structures with conductors above ground may be subject of a future paper.

Manuscript received May 3, 1994.